

Indexed by

Scopus®

## **PREDICTION THE SHEAR STRENGTH AND SHEAR MODULUS OF SAND-CLAY MIXTURE USING BENDER ELEMENT**

DOAJ  
DIRECTORY OF  
OPEN ACCESS  
JOURNALS

Crossref

**Badee Alshameri**  
National University of  
Sciences and Technology,  
Pakistan

ROAD  
DIRECTORY OF OPEN ACCESS  
RESEARCH RESOURCES

KoBSON

SCINDEKS  
Srpski citatni indeks

Google  
Scholar

**Key words:** sand-clay mixture, bender element, shear modulus, shear strength, maximum shear modulus

**doi:10.5937/jaes0-30619**

**Cite article:**

Alshameri B. (2022) PREDICTION THE SHEAR STRENGTH AND SHEAR MODULUS OF SAND-CLAY MIXTURE USING BENDER ELEMENT, *Journal of Applied Engineering Science*, 20(1), 168 - 176, DOI:10.5937/ jaes0-30619

**Online access** of full paper is available at: [www.engineeringscience.rs/browse-issues](http://www.engineeringscience.rs/browse-issues)

# PREDICTION THE SHEAR STRENGTH AND SHEAR MODULUS OF SAND-CLAY MIXTURE USING BENDER ELEMENT

**Badee Alshameri\***

**National University of Sciences and Technology, Pakistan**

*Employing the conventional laboratory geotechnical methods such as shear box test to measure shear strength and shear modulus require destroying the samples which is seen as time consuming and costly. Whilst the bender element technique (BE) maintains the sample condition, time, and cost efficiency. Several sand-clay mixtures were compacted and subjected to bender element test as well as sheared using shear box test to measure and correlate shear modulus ( $\tau$ ), shear strength ( $G$ ) and the maximum shear modulus ( $G_{max}$ ). The results showed the critical stage (transition fines-grained) at fine-grained (FG) equal to 50% where any further increment beyond this value led to decrement the soil mixture strength. Both  $\tau$  and  $G$  were normalized using moisture content, density, and applied normal stress. Five empirical equations from the normalized shear strength  $\tau N$  were applied on the previous field data to exam their reliable and limitations. The equations indicated the importance of including the effect of overburden pressure for the natural sample as well as the in-situ moisture content and field density to avoid uncertainty in the predicted value of the soil shear strength and modulus. At no depth limitation, all empirical equations ( $\tau N1$ ,  $\tau N2$ ,  $\tau N3$ ,  $\tau N4$ , and  $\tau N5$ ) exceed  $\pm 20\%$  lines which indicated a large variation in results. At depth limitation ( $< 5$  m), only one equation corresponding to  $N4$  showed reasonable validity and reliability to predict the shear strength. Similar was on the prediction of the shear modulus. The 5 m depth limit was recommended to apply the equation consistently.*

**Key words:** sand-clay mixture, bender element, shear modulus, shear strength, maximum shear modulus

## INTRODUCTION

The measurement of the shear strength and shear modulus is important in the engineering design. These parameters can be provided using several techniques: Modelling, Direct measurement, or Prediction through the empirical correlations. Numerous efforts have done to predict these parameters using numerical modelling. However, Hashemi and Rahmani [1], stated that there is a limitation associated with the numerical modelling (e.g. finite element method) related to mechanical properties of the soil. Using the conventional laboratory methods, as the shear box, to measure the strength parameters is the usual practice in the geotechnical engineering [2]. The process of this test consume time and costly compared with the seismic laboratory test. In addition, the sample from the shear box has a single use and cannot be reused. This is due to the destructive behaviour of the conventional geotechnical methods [3]. While the seismic laboratory test (i.e. bender element test) is a non-destructive method and the sample will remain intake [4,5]. The bender elements are plates made of a piezoelectric material which has the capability to either convert an applied electric voltage into mechanical motion or convert an applied mechanical motion into an eclectic voltage. Many researchers correlated the shear modulus at the small strain (i.e. maximum shear modulus) to different geotechnical parameters. Cabalar et al [6] used clay-sand mixtures to investigate the relation between the maximum shear modulus toward the sand content, size, and shape. Bahador and Pak [5] correlated the max-

imum shear modulus toward the applied pressure and moisture content using kaolinite-cement mixture. In Cabalar et al [6] and Bahador and Pak [5], the density of the mixture was ignored. Zeng and Ni [7] investigated the correlation between the maximum shear modulus and the applied pressure using sand. Ueno et al. [8] used the sandy soil to study the effect of the effective stress and the void ratio on the maximum shear modulus. Asadi et al. [9] and Choo et al. [10] studied the effect of the void ratio and the applied pressure toward the maximum shear modulus using the fly ash and sand, respectively. In Zeng and Ni [7]; Ueno et al. [8]; Asadi et al. [9] and Choo et al. [10] the effect of the moisture content and density were not considered. Yang and Lin [4]. Pintado et al. [11] and Sadeghzadegan et al. [12] used the residual lateritic soil, the bentonite and the sand-kaolinite mixture, respectively, to study the effect of the degree of saturation on the maximum shear modulus while density effect was not studied. Li et al. [13] focused on the correlation between the maximum modulus and density using polymer grouting materials. Qiu et al. [14] presented a good correlations between the maximum shear modulus toward both density and applied pressure. The effect of the fine-grained, void ratio and applied stress were studied separately by Wu et al. [15] using marine sand. Finally, Kulkarni et al. [16] compared the shear wave velocity and maximum shear modulus toward density, moisture content, applied pressure, and the undrained shear strength separately. However, no effort was done to combine and present the effects of density, moisture content, and applied pressure in one empirical correlation. Referring to

the aforesaid correlations, it can be indicated that a lot of efforts spent to develop separate correlations between individual soil parameters while no significant effort spent to correlate a combination of several soil parameters simultaneously toward the maximum shear modulus. Therefore, the bender element technique was used to correlate the maximum shear modulus toward of physical soil properties (shear strength and shear modulus) using a combination of applied stress, moisture content, and density simultaneously. Consequently, developing new empirical correlation equations to predict the shear strength ( $\tau$ ) and shear modulus ( $G$ ) from the bender element data [17,18].

## MATERIALS AND TEST PROCEDURES

### Geotechnical laboratory test

In this paper, 28 sand-clay mixture samples were distributed between six mixture groups which had fine-grained of 20, 30, 40, 50, 60, and 70%. The fine-grained material was kaolin with commercial named "AKIMA 45" which provided by Associated Kaolin Industries SDN BHD, Selangor Darul Ehsan, Malaysia with particle size ( $< 2 \mu\text{m}$ ) of 40% minimum, 325 mesh residues ( $45 \mu\text{m}$ ) of 0.05% maximum and packed in FIBC/Paper Bag. While the sand material has maximum particle size of 3.35 mm and the source was quarry on Jalan Minyak Beku, Batu Pahat city, Johor state, Malaysia. The particle size distribution for sand component on each FG is shown in Fig. 1. Each sample was compacted using three compacted layers in the 6-in. mould at method C in ASTM D689,[19] to determine the maximum dry density (MDD) and optimum moisture content (OMC) of the six groups of mixtures (see Table 1). All compacted samples were sheared under consolidated undrained conditions using shear box through method ASTM D3080 [3] to measure the shear strength and shear modulus [3,20–22]. The condition of the nature of seismic wave propagation effect on the soil particle (where the propagation of the seismic waves through the soil medium, cause sudden development in the stress without giving enough time to drain the water inside the voids) was simulated using the

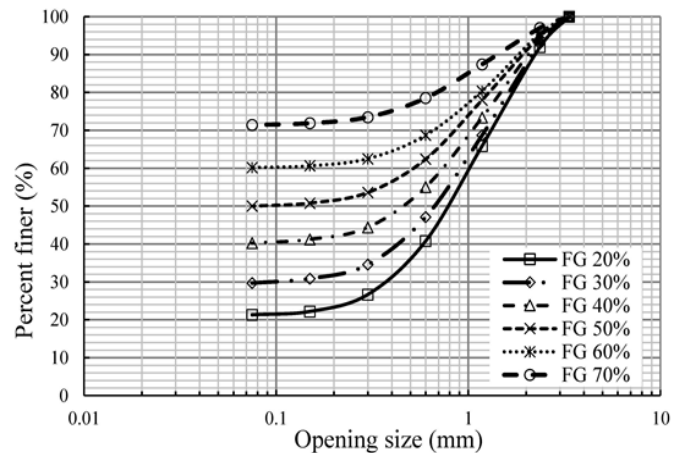


Figure 1: The particle size distribution of sand at the different FG

consolidated undrained direct shear methods through using the standard ASTM D3080 [3,23,24]. The relative high shear ratio (1 mm/min) represented the undrained condition on the direct shear test and avoided the water dissipation during the direct shear test. In the shear box test, three different applied normal stress (10.5, 21, and 31.5 kPa) were used in each sample with dimension of  $100 \times 100$  mm to avoid an overestimated result [3]. The specific gravity for the mixtures was determined using ASTM D854,[25]. The compactions curve (see Fig. 2) showed flatten pattern when the values of the fine-grained exceed 50%. At this value, the inter-granular void ratio will not dominate the behaviour of the mixture because the voids will be almost filled [26]. Further increment in the fine-grained will expands the distance between the sand particles. Thus, decrement the value of the maximum dry density compare with the compaction curves which had lower value of fine-grained and moisture content. Among 6 groups of the soil mixtures, only 9 representative soil samples were selected and subjected to the bender element test (Fig. 2). The selected 6 samples were compacted samples with FG ranging from 20 to 70% corresponding to the maximum dry density (MDD) and the optimum moisture content (OMC) whilst

Table 1: Properties of Mixtures

Fine-grained (clay content) FG %	Sand content %	Specific gravity	Dry density kg/m <sup>3</sup>	Moist density kg/m <sup>3</sup>	Moisture content %
70	30	2.553	1584	1901	20
60	40	2.563	1640	1935	18
50	50	2.576	1711	1985	16
40	60	2.585	1813	2030	12
30	70	2.597	1886	2112	12
20	80	2.61	1930	2162	12
20	80	2.61	1785	2071	16
50	50	2.576	1648	1846	12
60	40	2.563	1603	1860	16

three samples had FG equal to 20, 50, and 60 % with moisture content 12, 16, and 16%. These selected samples had moist density ranging of 2162 kg/m<sup>3</sup> to 1846 kg/m<sup>3</sup>.

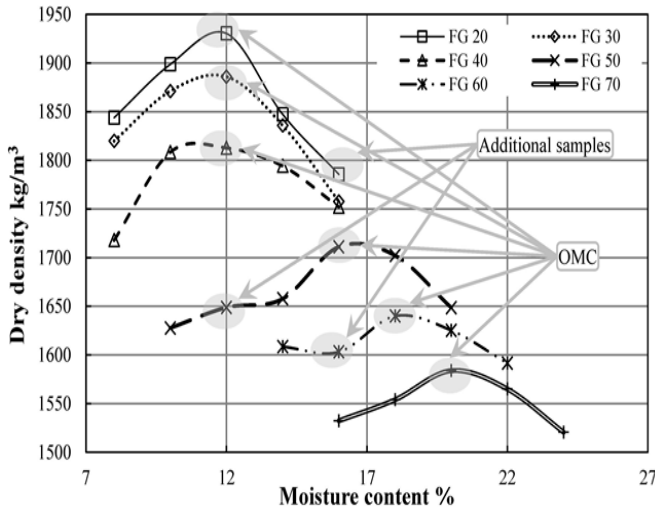


Figure 2: The selected soil mixture samples in bender element test

### Bender element test

A pair of bender elements with intruder length at 5 mm (supplied by Geotechnical Digital Systems Company, GDS company) was used to measure the shear wave velocity (VS) of sand-clay mixtures (see Fig. 3). 15 volts was used as input voltage, and all signals were subjected to 50 times stacking to increase the quality of the signal record by reducing the noise effect [27]. Five frequencies (30, 50, 100, 150, and 250 kHz) were applied in the bender element technique at each sample and the average is presented. The maximum shear modulus was calculated using equation 1:

$$G_{\max} = \rho V_S^2 \quad (1)$$

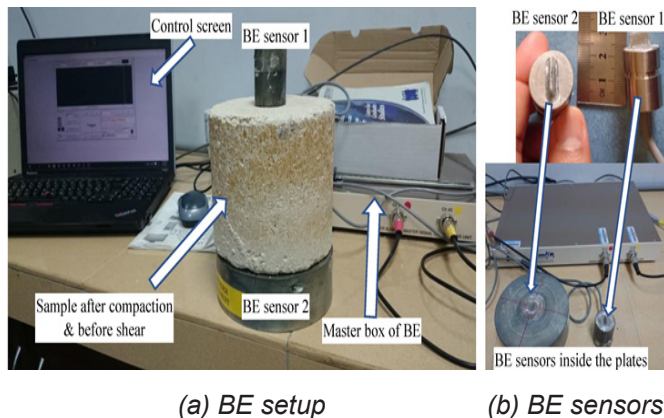


Figure 3: Bender element (BE) setup and sensors

where  $G_{\max}$  is the maximum shear modulus in Pa,  $\rho$  is the moist density in kg/m<sup>3</sup>,  $V_S$  is the seismic shear wave velocity in m/s. In the bender element test, the tip to tip distance was adopted in equation 2 to calculate the seismic wave velocity [28,29]. The bender element data was interpreted using both the first peak method and cross-correlation methods according to equation 3 [28,29]. In the first-peak method, the data were collected from the bender element software and then was subjected to the analysis using Microsoft Excel where the arrival time was calculated according to the differences between the first-peak in transmitter signal and the first-peak in the receiver signal. In the cross-correlation method, the travel time to be calculated as the function of differences between the two signals that have the highest value of similarity.

$$V = \frac{L_{tt}}{t} \quad (2)$$

$$CC_{xy}(t_s) = \frac{1}{T} \sum_{T=0}^{T-1} X(T)Y(T+t_s) \quad (3)$$

where  $V$  is the seismic wave velocity (either primary or shear wave velocities) in m/s,  $L_{tt}$  is the distance between the tip of transmitter sensor to tip of receiver sensor in m,  $t$  is the travel time in sec,  $CC_{xy}(t_s)$  is the time for maximum value of cross-correlation,  $t_s$  is the time shift for transmitter signal,  $Y(T)$  is transmitter signal and  $X(T)$  is the receiver signal.

## RESULTS AND DISCUSSIONS

### Geotechnical data

The shear strength and shear modulus data (using applied normal stress 21 kPa) were compared with fine-grained in Fig. 4. The results indicate an increase in both shear modulus and shear strength with an increase of fine-grained from 20% to 50%. Later, both shear strength and shear modulus decrement with further increment in the fine-grained (FG > 50%). At the first range, the fine-grained and moisture content were less than 50% and 16% respectively (see Table 1 Fig. 4) while the second range located at fine-grained and moisture content higher than 50% and 16% respectively. Referring to Fig. 4, it can indicate that the maximum value of the shear strength and shear modulus was achieved at value of 50% fine-grained then a further increment on the fine-grained led to decrement of the strength of the soil mixture [6,30]. This phenomena can be explained through the inter-granular void ratio aspect [31,32]. At lower value of the fine-grained, the soil strength will mainly depend on the frictions between the sand particles with less effect of cohesion forces. Later, with add more fine-grained, the kaolin will fill the voids and the integration between the fine-grained and moisture content will develop the cohesion force and adhesion forces to the soil structural, consequently, strengthen the soil [20,33]. This develop-

ing on the soil strength will continue in progress till all the voids filled. At this critical stage, a further increasing on the fine-grained and moisture content simultaneously will reverse the behaviour of the fine-grained and moisture content. Both fine-grained and moisture content will acting as lubricate agents and expand the distance between the sand particles causing decrement the internal friction between the sand particles as well as decrement the cohesion and adhesions forces due to extend the double-layer water [26,32]. In conclusion, weaken the soil structure then lowering soil strength. According to the results, the critical stage (transition fines-grained content) where the behaviour of the strength-composition overturned was achieved at fine-grained equal to 50 % [34].

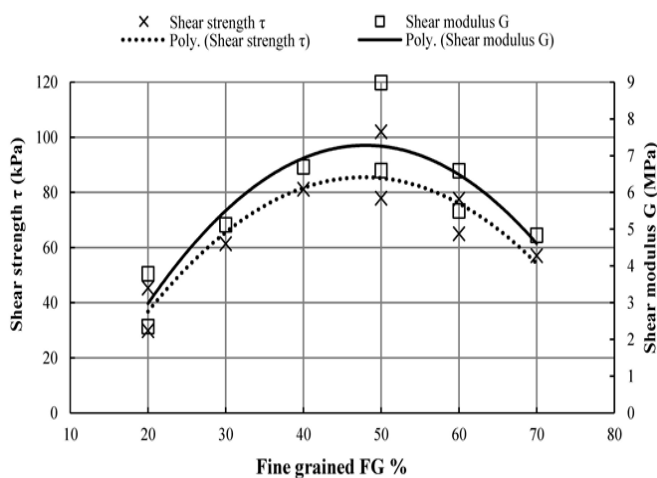


Figure 4: Shear strength and shear modulus at different fine-grained

**Prediction of physical soil properties using bender element test**

To improve the prediction of the shear strength ( $\tau$ ) using the bender element data (e.g. the maximum shear modulus  $G_{max}$ ), the shear strength was normalized using different geotechnical parameters [35]. Three geotechnical parameters which have an effect on the bender element data were used to normalize of; moisture content, density and applied normal stress [4,36]. The normalized shear strength ( $\tau_N$ ) was compared to the maximum shear modulus ( $G_{max}$ ) in Fig. 5 and equation 4 was used this comparison. The empirical correlation equations between the different normalized shear strength were summarized in Table 2. The moisture content effect, the applied normal stress as well as the density effect were ignored in the  $\tau_{N1}$  i.e. the shear strength was correlated directly of the maximum shear modulus. The effect of applied normal stress and density were considered in  $\tau_{N2}$  and  $\tau_{N4}$  while the effect of the moisture content was included in  $\tau_{N3}$  and  $\tau_{N4}$ . In  $\tau_{N5}$ , the effect of the density and moisture content without considering the applied normal stress and average moisture content in this study ( $w_0 = 0.15$ ).

$$\tau_N = B + AG_{max} \tag{4}$$

where A and B been calculated from Fig. 5,  $\tau$  is the shear strength in kPa, and  $G_{max}$  is the maximum shear modulus in MPa. The results in Fig. 5 showed lower R2 in  $\tau_{N3}$  and  $\tau_{N5}$  compare with  $\tau_{N1}$   $\tau_{N2}$  and  $\tau_{N4}$ . The range of  $G_{max}$  values from 120 MPa to 170 MPa, the  $\tau_{N1}$   $\tau_{N2}$ ,  $\tau_{N3}$  and  $\tau_{N5}$  showed high scatter due to ignoring the effect of the moisture content in  $\tau_{N1}$  and  $\tau_{N2}$  also the density at  $\tau_{N3}$  and the applied normal stress as well as the average moisture content in  $\tau_{N5}$ .

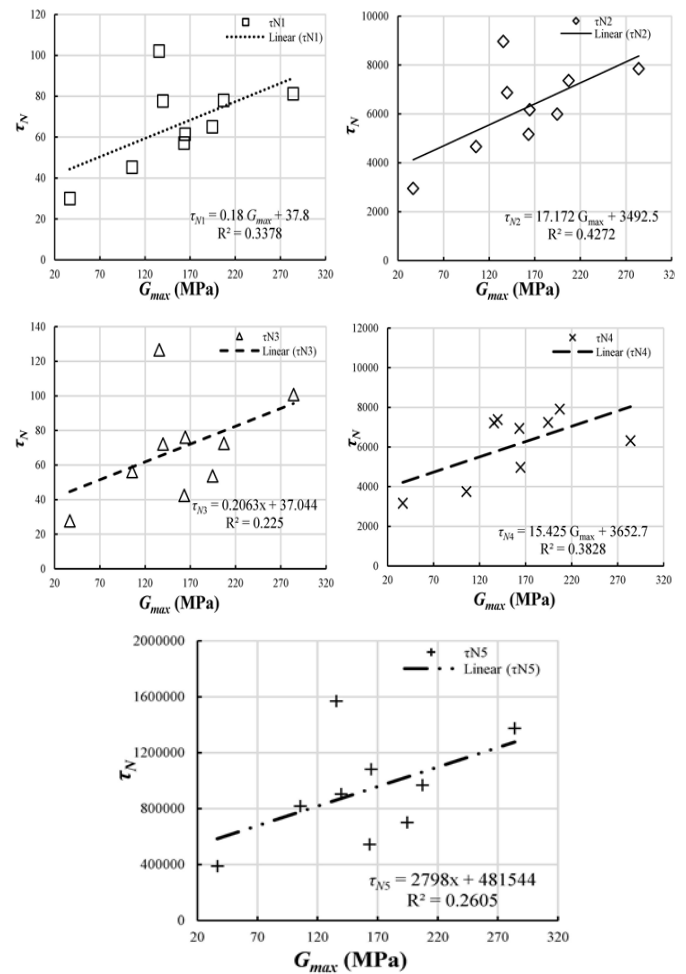


Figure 5:  $G_{max}$  versus  $\tau_N$  using different parameters

The five empirical correlation equations were applied on the field data of Kulkarni et al. [16] in Fig. 6 and Fig. 7. The samples on Kulkarni et al. [16] were undisturbed soil samples which collected from different locations at India coastal at depth of 0 m to 61 m. The samples contain different percentage of fractions (i.e. clay ranged from 7% to 78%, silt ranged from 8% to 87% and sand ranged from 0% to 51%). The samples had specific gravity ranged from 2.41 to 2.91, moisture content from 26.1 % to 128 % and density ranged from 1060 kg/m<sup>3</sup> to 2039 kg/m<sup>3</sup>. The limitation of the empirical equations was tested using two conditions (a) no depth limitation and (b) depth less than 5m. In the case of using no depth limitation, the predicted values of the shear strength indicate a high scatter in all the results of  $\tau_{N1}$ ,  $\tau_{N1}$   $\tau_{N3}$ ,  $\tau_{N4}$  and  $\tau_{N5}$  (see Fig. 6a). On the other hand, the scatter of

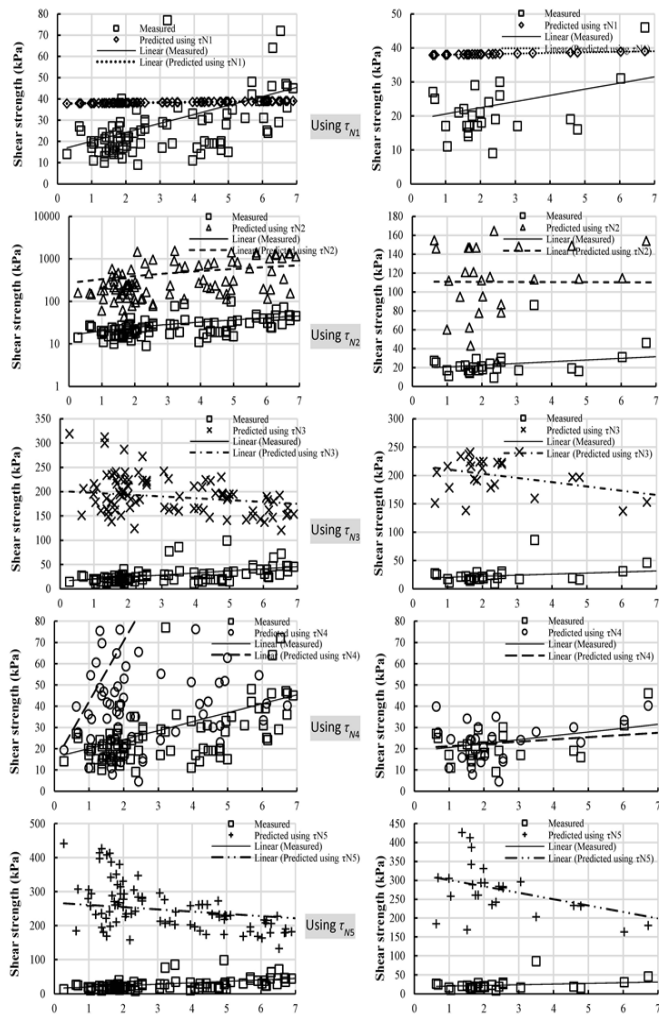
Table 2: Parameters of the empirical correlation equations of  $\tau$  versus  $G_{max}$

Normalized shear strength	Moisture content parameter wN	Density-Stress parameer LN	A	B
$\tau_{N1} = \tau$	-	-	0.180	37.8
$\tau_{N2}$	-	$\rho / \sigma$	17.17	3492.5
$\tau_{N3}$	w0 / w%	-	0.206	37.0
$\tau_{N4}$	w0 / w%	$\rho / \sigma$	15.425	3652.7
$\tau_{N5}$	w%	$\rho$	2798	481544.3

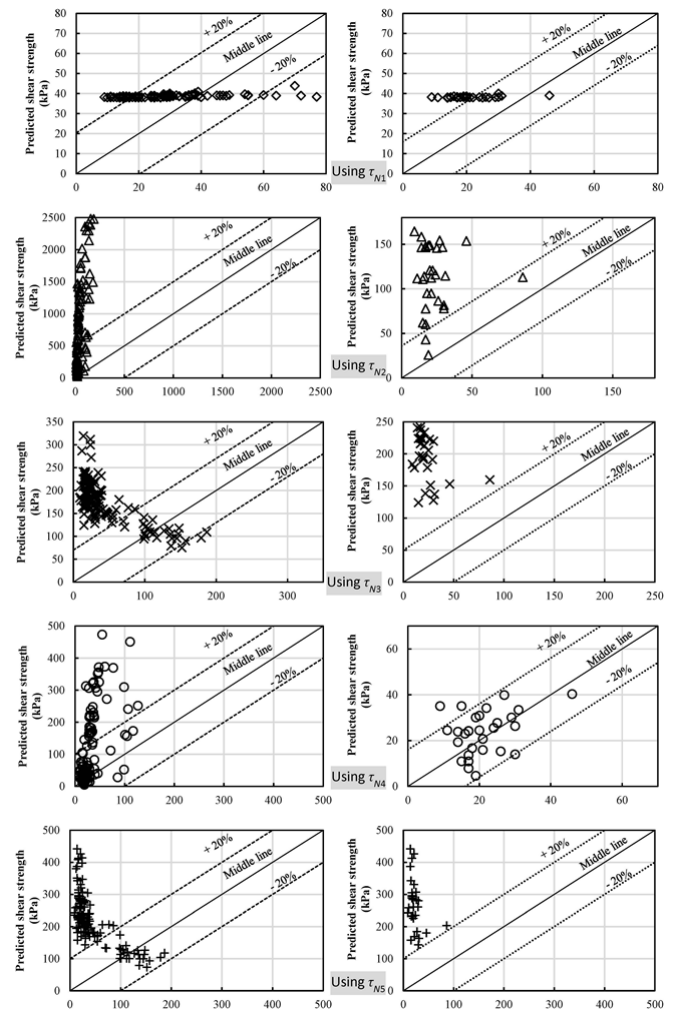
w% is the moisture content of the sample in %, w0% = 0.15 is the average moisture content of all sample in current research in %,  $\rho$  is the density of the sample in kg/m<sup>3</sup>,  $\sigma$  is the applied normal stress of the sample in kPa,  $\tau$  is the shear strength in kPa

the predicted values was reduced significantly when the limitation of the depth was considered (see Fig. 6b). In depth less than 5m, the  $\tau_{N1}$   $\tau_{N2}$ ,  $\tau_{N3}$  and  $\tau_{N4}$  showed overestimated results due not consider the moisture content, density and applied normal stress simultaneously. In contrast, considered the moisture content, density and applied normal stress simultaneously in  $\tau_{N4}$  provided clearly the most fit predicted results to the measured

compared with other equations. The predicted and measured shear strength values on the field data of Kulkarni et al. [16] was compared on the Fig. 7 to determine the variation in the results using the middle line and  $\pm 20\%$  line. At no depth limitation case, all equations  $\tau_{N1}$ ,  $\tau_{N2}$ ,  $\tau_{N3}$  and  $\tau_{N5}$  showed results extended from -20% line beyond the +20% line which indicated a large variation in results.



(a) No depth limitation (b) Less than 5 m depth  
Figure 6: Applying the empirical correlation equations on the field data of Kulkani et al. [16]



(a) No depth limitation (b) Less than 5 m depth  
Figure 7: Comparing the predicted and measured shear strength on the field data of Kulkarni et al. [16]

On other hands, applying the depth limitation (i.e. less than 5 m depth) provided a good fit with measured values for only equation τN4. The match between the predicted and measured shear strength through using equations τN4 (see Fig. 6b) was related to using, moisture conent, density and applied normal stress (see Table 2). In contrast, equations τN1 τN2, τN3 and τN5 showed no effect on the results as hypothesized due to said geotechnical parameters (w, ρ, and σ) (see Table 2). The normalized shear modulus (GN) was calculated according to equation 4 and using the same procedures as in the normalized shear strength (refer to Table 2) with replacing GN and G instead of τN and τ respectively. Fig. 8 showed the comparison between the normalized shear modulus and maximum shear modulus. Table 3 highlight the variation on the A and B while both moisture content parameter and density-stress parameter remined unchanged as in the normalized shear strength.

**Equations analysing, recommendation, and limitations**

The comparison between the predicted and measured values of the shear strength on the previous field work indicated the following; (a) equations 5, 6, 7 and 8 which corresponding to τN1, τN2, τN3 and τN5, respectively, always predict values higher than measured values of shear strength even with considering depth limitation. In equations τN5, the density and moisture content were considered but the predicted results showed a significant overestimation due to ignoring the effect of the applied normal stress on the equations τN5 which has a significant effect on the bender element [10,14]. Even in the conventional geotechnical test such as the direct shear, the shear strength of the sample will be affected by the applied normal stress [3]. Consequently, the variation on the predicted and measured shear strength will vary [37]. Obviously, the moisture content parameter will have a significant effect on the soil structural and soil strength as well as on the bender element data. This effect appeared clearly on the variation of the predicted results of equation 6 (using τN2) even with considering the applied normal stress and density. Equations 5 and 7 which corresponding to τN1 and τN3 showed a scatter results (refer to Fig. 6b) due to ignoring the effect of the density [14]

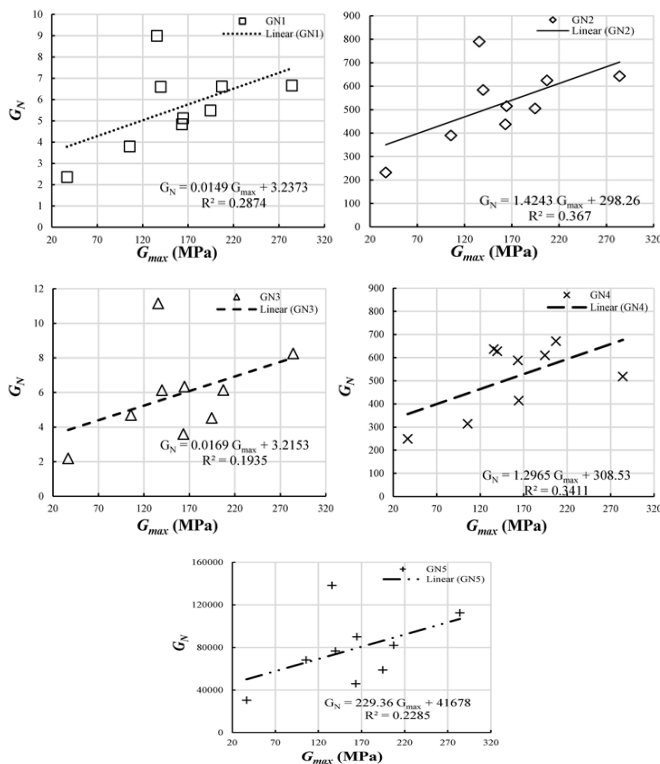


Figure 8: Gmax versus GN using different parameters

$$\tau = 37.8 + 0.18 G_{max} \quad \text{(using } \tau N1 \text{) (5)}$$

$$\tau = \frac{34.3 + 0.168 G_{max}}{L_N} = (34.3 + 0.168 G_{max}) \frac{\sigma}{\gamma} \quad \text{(using } \tau N2 \text{) (6)}$$

$$\tau = \frac{37 + 0.206 G_{max}}{W_N} = (37 + 0.206 G_{max}) \frac{w}{0.15} \quad \text{(using } \tau N3 \text{) (7)}$$

$$\tau = (4722.8 + 27.441 G_{max}) \frac{W_N}{L_N} = (4722.8 + 27.441 G_{max}) \frac{w}{\gamma} \quad \text{(using } \tau N5 \text{) (8)}$$

Where τ in kPa, Gmax in MPa, w is the moisture content of the sample in %, and ρ is the moist density of the sample in kg/m<sup>3</sup>. σ is the applied normal stress in kPa. In the equations 9 which were derived from τN4, the scatter in the predicted results was significantly reduced due to the use all the parameters of applied normal stress, the

Table 3. Parameters of the empirical correlation equations of G versus G<sub>max</sub>

Normalized shear modulus	Moisture content parameter wN	Density-Stress parameter LN	A	B
GN1 = G	-	-	0.0149	3.2373
GN2	-	ρ / σ	0.014	2.9252
GN3	w0 / w%	-	0.0169	3.2153
GN4	w0 / w%	ρ / σ	0.0127	3.0257
GN5	w%	ρ	2.2493	408.76

average moisture content, the moisture content, and the density in the normalized shear strength [7,10,14].

$$\tau = (35.8 + 0.151G_{max}) \frac{w_N}{L_N} = (35.8 + 0.151G_{max}) \frac{0.15\sigma}{w\gamma} \quad (\text{using } \tau_{N4}) \quad (9)$$

The comparison between the different equations and their accuracy and validity in Fig 6 and Fig 7 indicated the following:

- In case of no depth limitation, all equation equations 5, 6, 7, 8 to 9 which were derived from normalized shear strength  $\tau_{N1}$ ,  $\tau_{N2}$ ,  $\tau_{N3}$ ,  $\tau_{N4}$ , and  $\tau_{N5}$  failed to present a valid prediction for the shear strength even with consider all the geotechnical parameter such as moisture content, applied normal stress, and density,
- Equation 9 which were derived from normalized shear strength  $\tau_{N4}$  are reliable when the depth is less than 5 m (i.e. 5 times of applied normal stress corresponding to the value of density of the sample).
- According to the correlation and indication from normalized shear strength equation and their application, equation 9 which were derived from normalized shear modulus GN4 been assumed the reliable equation to predict the shear modulus with depth less than 5 m

$$\tau = (35.8 + 0.151G_{max}) \frac{w_N}{L_N} = (35.8 + 0.151G_{max}) \frac{0.15\sigma}{w\gamma} \quad (\text{using } \tau_{N4}) \quad (9)$$

Where the shear modulus (G) in MPa.

## CONCLUSIONS

Several sand-clay mixtures with different moisture content (8% to 24%) and fine-grained (20% to 70%) were compacted and subjected to bender element test as well as sheared on shear box test. The results indicated the following:

- The transition fines grained located at FG = 50%. Then the increment of both fine-grained and moisture content will lead to reduce the strength of the soil due to reduce the friction force between the sand particles as well as reduce the cohesion forces on the kaolin particles.
- The shear strength and shear modulus were normalized using three geotechnical parameters; moisture content, density, and applied normal stress.
- The results yielded five empirical correlation equations to predict the shear strength using maximum shear modulus from bender element data.
- The equations indicated the importance of including the effect of overburden pressure for the natural sample as well as the in-situ moisture content and field density to avoid uncertainty in the predicted value of the soil shear strength and modulus.
- At no depth limitation, all empirical equations ( $\tau_{N1}$ ,  $\tau_{N2}$ ,  $\tau_{N3}$ ,  $\tau_{N4}$ , and  $\tau_{N5}$ ) exceed  $\pm 20\%$  lines which indicated a large variation in results.

- At depth limitation (< 5 m), only equation 9 which were derived from normalized shear strength  $\tau_{N4}$  showed reasonable validity and reliability to predict the shear strength. Similar was on the prediction of the shear modulus.
- The present of the gravel or high plasticity clay can cause uncertainty on the predicted values. Consequently, it is recommended to use an extra combination of the other index soil properties (e.g. specific gravity, liquid limit, plastic limit) and use natural samples to increase the application and efficiency of the empirical equations.

## REFERENCES

- Hashemi, S. M., Rahmani, I. (2018). Determination of Multilayer Soil Strength Parameters Using Genetic Algorithm. Civil Engineering Journal, vol. 4, no. 10, 2383, DOI: 10.28991/cej-03091167.
- Alshameri, B., Bakar, I., Madun, A., Abdeldjouad, L., Dahlan, S. H. (2016). Effect of Coarse Materials Percentage in the Shear Strength. IOP Conference Series: Materials Science and Engineering, vol. 136, no. 1, DOI: 10.1088/1757-899X/136/1/012017.
- ASTM-D3080. (2012). Standard Test Method for Consolidated Undrained Direct Simple Shear Testing of Cohesive Soils. DOI: 10.1520/D3080.
- Yang, S. R., Lin, H. Da. (2009). Influence of soil suction on small-strain stiffness of compacted residual subgrade soil. Transportation Research Record, no. 2101, 63–71, DOI: 10.3141/2101-08.
- Bahador, M., Pak, A. (2012). Small-Strain Shear Modulus of Cement-Admixed Kaolinite. Geotechnical and Geological Engineering, vol. 30, no. 1, 163–171, DOI: 10.1007/s10706-011-9458-1.
- Cabalar, A. F., Khalaf, M. M., Karabash, Z. (2018). Shear modulus of clay-sand mixtures using bender element test. Acta Geotechnica Slovenica, vol. 15, no. 1, 3–15, DOI: 10.18690/actageotechslov.15.1.3-15.2018.
- Zeng, X., Ni, B. (1999). Stress-induced anisotropic Gmax of sands and its measurement. Journal of Geotechnical and Geoenvironmental Engineering, vol. 125, no. 9, 741–749, DOI: 10.1061/(ASCE)1090-0241(1999)125:9(741).
- Ueno, K., Kuroda, S., Hori, T., Tatsuoka, F. (2019). Elastic shear modulus variations during undrained cyclic loading and subsequent reconsolidation of saturated sandy soil. Soil Dynamics and Earthquake Engineering, vol. 116, 476–489, DOI: 10.1016/j.soildyn.2018.10.041.
- Asadi, M. B., Asadi, M. S., Orense, R. P., Pender, M. J. (2020). Small-Strain Stiffness of Natural Pumiceous Sand. Journal of Geotechnical and Geoenvironmental Engineering, vol. 146, no. 6, 06020006, DOI: 10.1061/(asce)gt.1943-5606.0002256.

10. Choo, H., Yeboah, N. N., Burns, S. E. (2016). Small to intermediate strain properties of fly ashes with various carbon and biomass contents. *Canadian Geotechnical Journal*, vol. 53, no. 1, 35–48, DOI: 10.1139/cgj-2014-0069.
11. Pintado, X., Romero, E., Suriol, J., Lloret, A., Madhusudhan, B. N. (2019). Small-strain shear stiffness of compacted bentonites for engineered barrier system. *Geomechanics for Energy and the Environment*, vol. 18, 1–12, DOI: 10.1016/j.gete.2018.12.001.
12. Sadeghzadegan, R., Naeini, S. A., Mirzaii, A. (2020). Effect of clay content on the small and mid to large strain shear modulus of an unsaturated sand. *European Journal of Environmental and Civil Engineering*, vol. 24, no. 5, 631–649, DOI: 10.1080/19648189.2017.1415169.
13. Li, J., Wang, B., Zhang, J. (2019). Study on precise measurement of shear modulus of polymer grouting materials using piezoceramic bender elements. *Tehnicki Vjesnik*, vol. 26, no. 3, 584–591, DOI: 10.17559/TV-20160205080600.
14. Qiu, T., Huang, Y., Guadalupe-Torres, Y., Baxter, C. D. P., Fox, P. J. (2015). Effective soil density for small-strain shear waves in saturated granular materials. *Journal of Geotechnical and Geoenvironmental Engineering*, vol. 141, no. 9, 1–11, DOI: 10.1061/(ASCE)GT.1943-5606.0001334.
15. Wu, Q., Lu, Q., Guo, Q., Zhao, K., Chen, P., Chen, G. (2020). Experimental investigation on small-strain stiffness of marine silty sand. *Journal of Marine Science and Engineering*, vol. 8, no. 5, 1–12, DOI: 10.3390/JMSE8050360.
16. Kulkarni, M. P., Patel, A., Singh, D. N. (2010). Application of shear wave velocity for characterizing clays from coastal regions. *KSCE Journal of Civil Engineering*, vol. 14, no. 3, 307–321, DOI: 10.1007/s12205-010-0307-1.
17. Roje-Bonacci, T., Mišćević, P., Salvezani, D. (2014). Non-destructive monitoring methods as indicators of damage cause on Cathedral of St. Lawrence in Trogir, Croatia. *Journal of Cultural Heritage*, vol. 15, no. 4, 424–431, DOI: 10.1016/j.culher.2013.07.008.
18. Foti, S., Lai, C., Rix, G. J., Strobbia, C. (2014). *Surface Wave Methods for Near-Surface Site Characterization*. Taylor & Francis Group, LLC, London, DOI: 10.1201/b17268.
19. ASTM-D698. (2012). *Standard Test Methods for Laboratory Compaction Characteristics of Soil Using Standard Effort (12400 ft-lbf/ft<sup>3</sup> (600 kN-m/m<sup>3</sup>))*. West Conshohocken, PA, DOI: 10.1520/D0698-12E01.1.
20. Alshameri, B., Madun, A., Bakar, I. (2017). Assessment on the effect of fine content and moisture content towards shear strength. *Geotechnical Engineering*, vol. 48, no. 4, 76–86, .
21. Alshameri, B., Madun, A., Bakar, I. (2017). Comparison of the Effect of Fine Content and Density towards the Shear Strength Parameters. *Geotechnical Engineering*, vol. 48, no. 2, 104–110, .
22. ASTM-D6528. (2007). *Standard Test Method for Consolidated Undrained Direct Simple Shear Testing of Cohesive Soils*. West Conshohocken, PA, USA, DOI: 10.1520/D6528-07.
23. Lillie, R. J. (1999). *Whole Earth Geophysics : An Introductory Textbook for*. Prentice Hall Upper Saddle River, New Jersey, USA, .
24. Telford, W. M., Geldart, L. P., Sheriff, R. E. (1990). *Applied geophysics*. 2nd ed. Press Syndicate of the University of Cambridge, Melbourne, Australia, . <http://linkinghub.elsevier.com/retrieve/pii/003192019190163C>.
25. ASTM-D854. (2010). *Standard Test for Specific Gravity of Soil Solids by Water Pycnometer*. West Conshohocken, PA, USA, DOI: 10.1520/D0854-10.
26. [26]Alshameri, B. (2020). Maximum dry density of sand–kaolin mixtures predicted by using fine content and specific gravity. *SN Applied Sciences*, vol. 2, no. 10, 1693, DOI: 10.1007/s42452-020-03481-9.
27. Khan, M., Liu, Y., Farid, A., Owais, M. (2018). Characterizing Seismo-stratigraphic and Structural Framework of Late Cretaceous-Recent succession of offshore Indus Pakistan. *Open Geosciences*, vol. 10, no. 1, 174–191, DOI: <https://doi.org/10.1515/geo-2018-0014>.
28. Alshameri, B., Madun, A., Bakar, I., Mohamad, E. T. (2015). Effect of Sensor Rotation on Assessment of Bender Element Apparatus. *Jurnal Teknologi*, vol. 77, no. 11, 51–57, DOI: 10.11113/jt.v77.6420.
29. Alshameri, B., Bakar, I., Madun, A., Mohamad, E. T. (2015). Effect of Alignment on the Quality of Bender Element Procedure. *Jurnal Teknologi*, vol. 76, no. 2, 73–80, DOI: 10.11113/jt.v76.5436.
30. Cabalar, A. F., Demir, S., Khalaf, M. M. (2019). Liquefaction resistance of different size/shape sand-clay mixtures using a pair of Bender element-mounted molds. *Journal of Testing and Evaluation*, vol. 49, no. 1, 509–524, DOI: 10.1520/JTE20180677.
31. Mitchell, J. K., Soga, K. (2005). *Fundamentals of soil behavior*. 3rd ed. John Wiley & Sons, Inc, New Jersey, USA, .

32. Belkhatir, M., Arab, A., Della, N., Missoum, H., Schanz, T. (2010). Influence of inter-granular void ratio on monotonic and cyclic undrained shear response of sandy soils. *Comptes Rendus - Mécanique*, vol. 338, no. 5, 290–303, DOI: 10.1016/j.crme.2010.04.002.
33. Alshameri, B., Madun, A. (2019). Comprehensive Correlations Between the Geotechnical and Seismic Data Conducted via Bender Element. *Geotechnical and Geological Engineering*, vol. 37, no. 6, 5077–5095, DOI: 10.1007/s10706-019-00963-5.
34. Cabalar, A. F., Mustafa, W. S. (2017). Behaviour of sand–clay mixtures for road pavement subgrade. *International Journal of Pavement Engineering*, vol. 18, no. 8, 714–726, DOI: 10.1080/10298436.2015.1121782.
35. Robertson, P. K., Sasitharan, S., Cunning, J. C., Segoo, D. C. (1995). Shear-wave velocity to evaluate in-situ state of Ottawa sand. *Journal of Geotechnical Engineering*, vol. 121, no. 3, 262–273, DOI: 10.1061/(ASCE)0733-9410(1995)121:3(262).
36. Francisca, F., Yun, T. S., Ruppel, C., Santamarina, J. C. (2005). Geophysical and geotechnical properties of near-seafloor sediments in the northern Gulf of Mexico gas hydrate province. *Earth and Planetary Science Letters*, vol. 237, no. 3–4, 924–939, DOI: 10.1016/j.epsl.2005.06.050.
37. Mohamad, E. T., Alshameri, B., Kassim, K. A., Saad, R. (2011). Shear strength behaviour for older alluvium under different moisture content. *Electronic Journal of Geotechnical Engineering*, vol. 16 F, 605–617, .

*Paper submitted: 30.01.2021.*

*Paper accepted: 18.04.2021.*

*This is an open access article distributed under the  
CC BY 4.0 terms and conditions.*